
SE-MoE: A SCALABLE AND EFFICIENT MIXTURE-OF-EXPERTS DISTRIBUTED TRAINING AND INFERENCE SYSTEM

Liang Shen Zhihua Wu WeiBao Gong Hongxiang Hao Yangfan Bai HuaChao Wu

Xinxuan Wu Jiang Bian Haoyi Xiong Dianhai Yu Yanjun Ma

Baidu Inc

ABSTRACT

With the increasing diversity of ML infrastructures nowadays, distributed training over heterogeneous computing systems is desired to facilitate the production of big models. Mixture-of-Experts (MoE) models have been proposed to lower the cost of training subject to the overall size of models/data through gating and parallelism in a divide-and-conquer fashion. While DeepSpeed has made efforts in carrying out large-scale MoE training over heterogeneous infrastructures, the efficiency of training and inference could be further improved from several system aspects, including load balancing, communication/computation efficiency, and memory footprint limits. In this work, we present SE-MoE that proposes *Elastic MoE training* with *2D prefetch* and *Fusion communication* over *Hierarchical storage*, so as to enjoy efficient parallelisms in various types. For scalable inference in a single node, especially when the model size is larger than GPU memory, SE-MoE forms the CPU-GPU memory jointly into a ring of sections to load the model, and executes the computation tasks across the memory sections in a round-robin manner for efficient inference. We carried out extensive experiments to evaluate SE-MoE, where SE-MoE successfully trains a Unified Feature Optimization (UFO) model with a Sparsely-Gated Mixture-of-Experts model of 12B parameters in 8 days on 48 A100 GPU cards. The comparison against the state-of-the-art shows that SE-MoE outperformed DeepSpeed with 33% higher throughput (tokens per second) in training and 13% higher throughput in inference in general. Particularly, under unbalanced MoE Tasks, e.g., UFO, SE-MoE achieved 64% higher throughput with 18% lower memory footprints. The code of the framework will be released on: <https://github.com/PaddlePaddle/Paddle>.

Keywords MoE Training · MoE Inference · Efficient · Storage

1 Introduction

In recent years, large-scale neural networks have excelled in many machine learning tasks, such as natural language processing(NLP) [1, 2, 3] and computer vision(CV) [4]. At the same time, the parameter scale of the model has expanded from tens of billions of parameters, such as the GPT-3 model with 175B parameters [2, 5], Ernie3.0 Titan with 260B parameters [6] and Megatron-Turing NLG with 530B parameters [7]. However, these densely activated models require abundant computing resources and massive training time. Simultaneously, the inference performance of the super large-scale models is difficult to satisfy the actual demands. For example, by December 2021, the largest single densely activated model, Megatron-Turing NLG with 530B, had taken 3 months to train on over 2000 NVIDIA A100 GPUs [7], making it more costly and further prevent from developing into a model with a larger parameter scale.

To optimize training for large-scale models, the Click-Through Rate(CTR) prediction [8] model contains numerous sparse feature embeddings to exploit the huge parameters [9]. However, it only utilizes one special layer to process high-dimensional input data to scale up the model. Beyond that, differently from the densely activated models, multi-task learning [10] is proposed in pre-trained language models [11, 12, 13] about multilingual neural machine translation.

Nevertheless, these methods require numerous computing resources to obtain state-of-the-art models. To solve the above issues [14, 15, 16], the sparsely activated neural networks based on Mixture-of-Experts(MoE) are proposed to train larger models with limited or no additional computing resources and achieve better training effects. The MoE architecture selectively activates a subset of parameters for training according to the input data in comparison with the densely activated models. Given the sparsity, the computing cost increases sub-linearly concerning the size of the model. For example, the largest version of GLaM [17] has 1.2T parameters and 64 experts per MoE layer in total, but each token from the input batch activates only a subnet of 95B (8% of 1.2T) parameters. And compared with the training GPT-3(175B), two-thirds of the electricity cost is saved, and only half of the computing resources are required in inference. Despite all the benefits, MoE models present their challenges and limitations in computation, communication, and storage.

1.1 Computation Challenges

Although the computing cost remains constant when the parameter scale gets expanded due to the increase of experts, computation in training and inference is confronted with the following limitations. On the one hand, MoE tends to make the training effects worse because of the imbalance in expert selection [16]. Therefore, many solutions have been proposed, such as adding auxiliary loss [15], using stochastic experts [18] and the noisy routing strategy [16]. Besides limiting the capacity of experts, it can also avoid inefficient training and the waste of computing resources. On the other hand, the calculation of routing selection and auxiliary loss at each layer pays more attention to scheduling than computing, which takes more burden to CPU devices without reusing high-speed computing devices such as GPU. At the same time, there are a lot of redundant operations introduced to the computation, such as Host2Device(H2D) and Device2Host(D2H) [19].

1.2 Communication Challenges

Most of the ongoing research has paid more attention to the imbalance of routing strategies caused by the gating network learning [14, 15, 16, 20]. However, because the activation of parameters in MoE is very closely interrelated to the input data, the notorious load imbalance often occurs when the data is unbalanced despite the efficient routing methods. For cross-device communication, the load imbalance results in the inconsistent pace of each device, causing mutual waiting for synchronous communication, especially in multi-task training. At the same time, taking Switch Transformer [16] as an example, each MoE layer requires AlltoAll communication for four times in both forward and backward stages, which frequently cross nodes or clusters. When the underlying network topology cannot be perceived, inter-machine communication is more prone to routing conflict and blocking, causing rapid performance degradation.

1.3 Storage Limitations

The MoE architectures is significantly limited by memory storage in computing devices. For densely activated models, the model scale is often restricted by the training time rather than memory. For example, the dense model with 1 trillion parameters takes around 3 months to train 450 billion tokens with 3072 A100 GPUs [5]. In contrast, the MoE model with trillions of parameters only requires a few weeks for training the same amount of tokens because its computing cost increases sub-linearly. However, the model scale depends on whether the device memory endures the occupation of model states. Although all available storage of the devices contains High-Bandwidth Memory(HBM) [21] in GPUs, CPU Memory, SSDs(solid-state-drives) and so on, the I/O latency among them is different from each other, making computation wait for parameter and others. It is challenging to construct a unified and efficient storage management to support sparsely activated training to break the memory wall.

1.4 Proposed Solution

This paper introduces a novel unified framework based on a open-source platform for MoE training and inference, which outperforms the state-of-the-art dense model on NLP and CV tasks. To overcome the challenges and limitations of MoE, some related research papers (Section 6) are presented, and their insights are optimized:

- A novel distributed system named SE-MoE, capable of scaling MoE models to trillions of parameters, fully utilizes the clusters including HBM, CPU memory and even SSDs to go beyond the memory wall and achieves efficient training scheduling. Moreover, using 2D prefetch scheduling and fusion communication are to improve heterogeneous storage efficiency (Section 2).
- A new inference method based on the ring memory is employed by dynamic graph scheduling, which can overlap the computation and communication as much as possible and further obtain more efficient inference performance without using additional machines for larger-scale MoE models (Section 3).

- Some effective training methods to scale up multi-task learning without extra memory and improve performance are employed by SE-MoE in NLP and CV tasks. These methods include load balancing, embedding partition, and resource-aware communication (Section 4).

The training and inference performance of models with different scales is our concern and the effective training recipes are adopted to train the CV task called UFO. Details about the experiments are presented in Section 5.

2 MoE Training Design

In the field of deep learning, there are two key factors affecting the performance and effect of model training: the model scale and the data size. It’s quite a challenge for all scientific institutions and enterprises to explore further due to the requirements of massive resources for computation and storage. To solve this problem, a new training method has been proposed and introduced to the industry in recent years. Different from the densely activated model putting all the parameters into computation, the sparsely activated model adaptively selects a subset of its parameters for training according to the input data, and the parameters can be increased linearly without increasing the amount of calculation, which make larger models based on MoE architecture more feasible and efficient.

To train models with considerable parameters with as few hardware resources as possible, it’s an appropriate solution to adopt the offloading strategy and train larger-scale models with the extreme utilization of storage resources in devices. Recently, DeepSpeed has presented an efficient method named Zero-infinity [22] and trained over 30 trillion parameters using 512 V100 GPUs in NVIDIA DGX-2 nodes. This method breaks through the limitation of memory and enables training of a super large-scale model on one single device by making full use of the storage space including High Bandwidth Memory(HBM) in GPU, CPU memory, and SSDs. Meanwhile, both the Zero strategy [23, 22] and the parameter prefetching strategy are applied to the reduction of storage occupation and the improvement of the training performance respectively. However, SSDs have a limited lifetime number of writes, and also slow down as they reach their full storage capacity [24].

There’s an optimization solution of MoE training that is proposed to solve the problems of SSDs and the scheduling in the large model training. Firstly, the parameters of the MoE model are classified into two categories according to the properties of activation: one is the sparse parameters, which are selectively activated in the training, such as expert parameters in switching FFN layer; the other is the dense parameters, which are always activated during the training, such as parameters in the multi-head attention layer. Generally, the sparse parameters account for a large proportion in MoE model easily tends to break the limitation of GPU storage. Then, as shown in Figure 1, we specifically redesign the architecture of the MoE training system, by combining various storage devices for abundant memory of sparse and dense parameters. At the same time, to alleviate the degradation of training performance caused by movement between different devices, we propose a creative strategy named 2D prefetch scheduling. In the following, we will introduce our training design in detail by three aspects as hierarchical storage, 2D prefetch scheduling and fusion communication.

2.1 Hierarchical Storage

In large-scale MoE models, as the parameter scale increases, storage has become a major bottleneck in model training. Normally the stored parameter states consist of three parts: the trainable parameters, the gradients of parameter, and the corresponding optimizer states. According to the different storage mediums, the storage device can be classified into three parts to store the parameter states: GPU-Node, CPU-Node, and SSD-Node. Because dense parameters are intensively used for computation and do not account for the majority of storage space, their parameter states are all stored on the GPU-Node to avoid frequent data movement. In contrast, since sparse parameters are selectively activated in training and occupy a lot of storage space compared with dense parameters, the parameter states are placed on SSD-Node and transported to GPU-Node at the appropriate time for calculation. By reasonably storing the corresponding parameter states on hierarchical storage according to the calculation and storage characteristics of parameters, the storage of devices can be fully utilized as much as possible.

In addition, considering the limit of storage nodes, we give several theoretical storage formulas to describe the relationship between each storage device and the storage parameter states with ADAM [25]. By default, there are eight GPUs per device. Supposing that D and S respectively represent the total number of dense parameters and sparse parameters, and L represents MoE layers’ numbers. Then, the total size of SSD memory, CPU memory and GPU memory on one device is M_{SSD} , M_{CPU} and M_{GPU} respectively. Next, N represents the number of devices, and we use α to describe the probability of sparse parameter being activated on the whole training process, where $0 \leq \alpha \leq 1$. For the GPU-Node, it stores the dense parameter states used in forward propagation(FWD), backward propagation(BWD) and parameter updating (param fp16, grad fp16, master param fp32, momentum fp32, variance fp32, $2D+2D+2D+2D+4D=16D$ bytes), sparse parameters and sparse parameter gradients($2\alpha S/L+2\alpha S/L=4\alpha S/L$

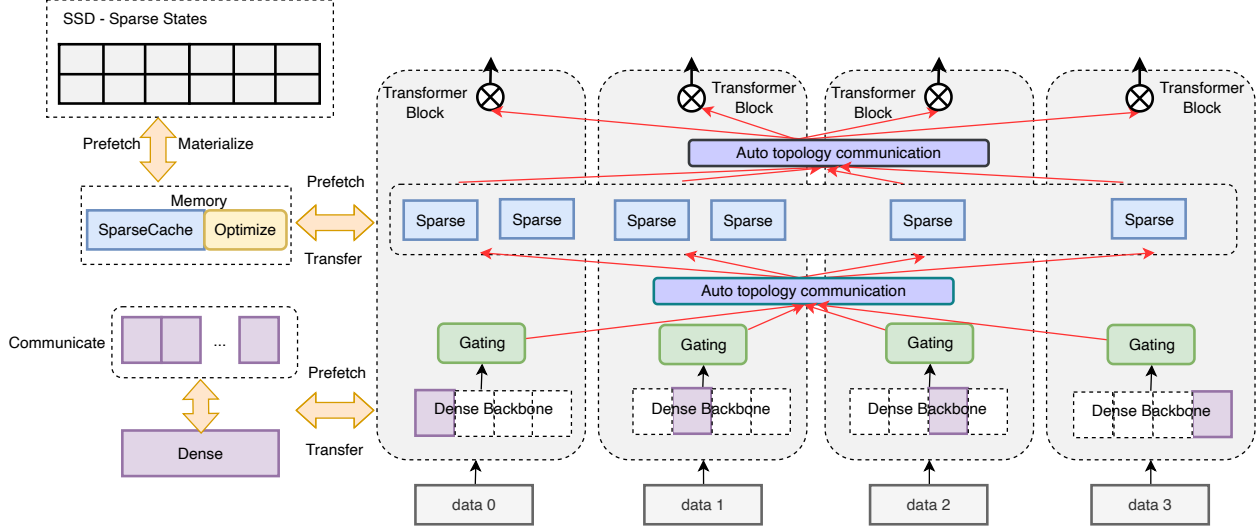


Figure 1: Overall MoE training: This is an example of the MoE training with four devices. According to the parameter state property of MoE model, the parameter states are stored in GPU and SSD respectively. With this heterogeneous storage, NVLink and PCIe bandwidth can be used at a time in two dimensions.

bytes). The CPU-Node is used as the cache to hold the high-frequency sparse parameter states($16\alpha S$ bytes), and the SSD-Node is used to store all the sparse parameter states in the device(master param fp32, momentum fp32, variance fp32, $12S$ bytes).

$$\begin{aligned}
 \text{GPU-Node} : \quad & 16D + 4\alpha S/L \leq M_{GPU} \cdot N \\
 \text{CPU-Node} : \quad & 16\alpha S \leq M_{CPU} \cdot N \\
 \text{SSD-Node} : \quad & 12S \leq M_{SSD} \cdot N
 \end{aligned} \tag{1}$$

The scale of the entire MoE model is:

$$P = S + D \tag{2}$$

As described above, the sparse parameters are stored in SSDs as files. Because of the limitation of the flash mediums, PCIe bandwidth and NVMe protocol, SSDs have high latency and finite frequency of erasures. It is challenging to utilize SSDs under the scenario of MoE training with frequent writing operations. To avoid this problem, we further turn our attention to Intel Optane Persistent Memory(Optane PMem) [26] which is a new storage medium that can provide byte addressing like DRAM and persistent storage like SSDs. Optane PMem connects to the integrated memory controller(IMC) of CPU through the DIMM(Dual Inline Memory Module) interface, and uses DDR-T(A protocol on top of the electrical/mechanical interface for DDR4) for communication. It supports byte-wise addressing using CPU instructions to achieve higher bandwidth and lower latency. Besides, Optane PMem provides two modes: memory mode and AppDirect mode. Because we only need to store the parameter files in the Optane PMem, we choose AppDirect mode and configure the namespace type as FSDAX. With the help of Ext4, we can use load/storing directly access to the GPU bypass page cache and kernel, without any interruptions and context switches.

2.2 2D Prefetch Scheduling

Since we adopt hierarchical storage to save the sparse parameter states and dense parameter states, it costs significantly growing time to transfer parameter states between different devices during MoE training. Therefore, we propose a 2D prefetch scheduling strategy and apply it to MoE training so that the computation of parameters can be overlapped with the scheduling as shown in Algorithm 1. For the dense parameter slice after using the zero-3 strategy, as shown in Figure 1, the complete dense parameters can be prefetched after communication among the ranks in the horizontal dimension through the high-speed bandwidth of NVLink, accomplishing the desired effect of data parallelism. Similarly, sparse parameters can be prefetched through PCIe bandwidth in the vertical dimension of the device. Considering that sparse parameters are stored in SSDs, we reduce the sparse parameter states access to the SSDs and establish the corresponding cache mechanism in the CPU memory like LRU mechanism [27]. The CPU caches are responsible for storing the selectively activated sparse parameter states used for FWD/BWD calculation and parameter updating. When

Algorithm 1: 2D Prefetch Scheduling Algorithm

Data: p_s : Sparse parameter states
 d_{slice} : Dense parameter state slices
 $caches_{cpu}$: CPU caches
 CPU_{size} : The size of sparse parameter states that the CPU can cache
 $hits$: The hit times of sparse parameter on hash table
 $threshold$: Hit threshold
 β : Attenuation coefficient
 K : Moving average steps
 $steps = 0$: Cycle steps
 $acc_{caches} = 0$: Cumulative caches ▷ Record the number of sparse parameters on CPU

1 Function DenseSchedule():
2 | Do *AllGather*(d_{slice}) ▷ Get total parameters in next layers
3 End Function

4 Function SparseSchedule():
5 | **if** p_s in $caches_{cpu}$ **then**
6 | | Get p_s from $caches_{cpu}$
7 | | $hits[p_s] += 1$
8 | **else if** $acc_{caches} + 1 < CPU_{size}$ **then**
9 | | $hits[p_s] = 1$
10 | | $acc_{caches} += 1$
11 | | Fetch p_s from SSDs to $caches_{cpu}$
12 | **else**
13 | | **foreach** p_a in $hits$ **do**
14 | | | $hit_a = hits[p_a]$
15 | | | **if** $hit_a \geq threshold$ and $\min(hits.values()) == hit_a$ **then**
16 | | | | Update the states of p_a on SSDs
17 | | | | Delete the states of p_a in $caches_{cpu}$
18 | | | | Delete $hits[p_a]$
19 | | | | Fetch p_s from SSDs to $caches_{cpu}$
20 | | $steps += 1$
21 | | **if** $steps == K$ **then**
22 | | | $hits \cdot \beta$ ▷ Moving average
23 | | | $steps = 0$
24 | | $p_s \rightarrow GPU$ ▷ Transfer p_s to the corresponding GPU
25 End Function

26 Do in parallel
27 | DenseSchedule()
28 | SparseSchedule()
29 | Do FWD/BWD calculation ▷ Use the current parameter states to do FWD/BWD calculation
30 End Parallel

a prefetch request is received, it is preferred to retrieve the requested sparse parameters from the CPU caches, and then retrieve them from the SSDs if they are not stored in the CPU caches. When the CPU caches are full or reach the sparse parameter update cycle period, we use sparse parameters states from the CPU caches to update the corresponding parameters states on SSDs.

Because the CPU memory of each machine only caches some frequently activated sparse parameters, we only need to prefetch the parameters of the one or more expert layers, which are cached on the CPU memory, to the corresponding GPU memory in advance. By prefetching parameters in advance, the waiting time of computation can be greatly reduced. From a global perspective, through the bandwidth of NVLink and PCIe in two dimensions, we can prefetch dense and sparse parameters at the same time to reduce the scheduling gap caused by heterogeneous storage and greatly increase the training efficiency.

Next, as shown in Algorithm 1, we will introduce the CPU cache mechanism in detail. We additionally maintain the historical hit information of each sparse parameter, which is recorded as a hash table called *hits*. Specifically, if the

parameter p_s is requested, and it has been used in the previous FWD, we raise its count in the *hits*. If the CPU caches have reached the maximum limitation, we update the sparse parameter states which have the lowest hit frequency and exceed the hit threshold. Then we release them and move the states of parameter p_s from SSDs to the CPU caches. With every K training steps, we use moving average optimization to balance the hit frequency of each sparse parameter and increase the efficiency of CPU caches.

2.3 Fusion Communication

Fusion parameters: As previously described in 2D prefetch scheduling, we use Zero-3 data parallelism [22] for dense parameters. Meanwhile, multiple-time communication is requested in FWD and BWD calculation of MoE training, which increases the scheduling intervals in the training and thus affects the training efficiency. To reduce discontinuous communication, we adopt the fusion strategy for the parameters which are requested communication. Through the parameter management unit, parameter slices can be combined into a larger one before communication, and then cut into corresponding smaller ones after communication. As shown in Figure 2a, we manage the current parameter slices on each rank and fuse them as needed. After communication, we rebuild the whole parameter states according to the recorded slice index. By decreasing times of communication, the reduced latency overhead allows better scaling to numerous devices.

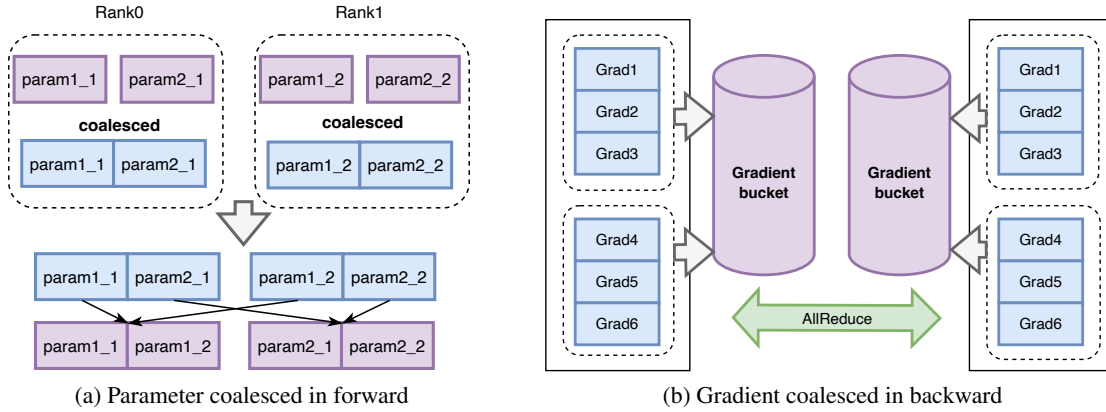


Figure 2: Fusion communication of dense parameters and gradients

Gradient Buckets: In backward propagation, one-by-one gradient communication will undoubtedly cause increasing times of communication operations and raise the blank time of communication. At the same time, there will be potentially probability of disordered communication between different ranks. To avoid the above-mentioned problems, we build a bucket unit especially for gradient communication [23]. As shown in Figure 2b, we apply for the bucket space in advance, which can accommodate the gradients of N parameters. The communication unit will not be triggered until all the backward propagation about parameters involved in the bucket is finished. Backward communication through gradient buckets can largely avoid inconsistent gradient aggregation order and reduce the generation of GPU memory fragments, which can improve GPU memory utilization.

3 MoE Inference Design

There has been lots of research [17, 28] showing that MoE models are significantly more efficient to train than dense models. However, for inference, numerous parameters (mostly ineffective parameters) introduce a larger storage burden compared to the dense model. For one thing, knowledge distillation [16, 29, 30, 31] is popular in the reduction of model size and accuracy preservation. DeepSpeed [32] has proposed Mixture-of-Students(MoS) architecture to enhance student model accuracy. For another thing, to achieve low latency and high throughput at a large scale for MoE, diverse parallelism techniques are designed [32], including expert-slicing, expert parallelism, tensor-slicing, and so on. However, multiple storage devices are not considered in the inference of MoE at an unprecedented scale when the number of machines is delimited. Below, for SE-MoE, we introduce an assembled process from train to inference deployment to achieve the purpose of high efficiency and low carbon. And we show innovations in the MoE inference architecture based on ring memory that supports inference to go beyond the memory wall and maintain efficient performance as much as possible.

3.1 Efficient Inference on MoE

The training part of SE-MoE adopts dynamic graph training, which has predominant debugging and flexibility. In contrast, to achieve stability and efficiency, the static graph is used in the inference and deployment stage. As shown in Figure 3, the whole inference process is divided into six steps: (1) Graph Fusion. For the model of ultra-large-scale distributed training, the origin graph is merged with the corresponding distributed strategy, which is employed in parameter redundancy elimination. (2) Distillation and Compression. Compress the numerous experts of the teacher network through distillation and compression to get the student network with fewer experts. (3) Graph Conversion. Convert the dynamic graph into a static graph for subsequent optimization and deployment. (4) Graph Segmentation. According to inference resources and the actual demand, a rational distributed strategy has been chosen manually or automatically to split the static graph into multiple distributed sub-graphs and add extra communication. (5) Optimization. For the distributed sub-graphs, pertinent IR Pass optimization like kernel fusion is used to further ameliorate the performance of inference. (6) Deployment. Deploy the optimized sub-graphs to the server to provide service.

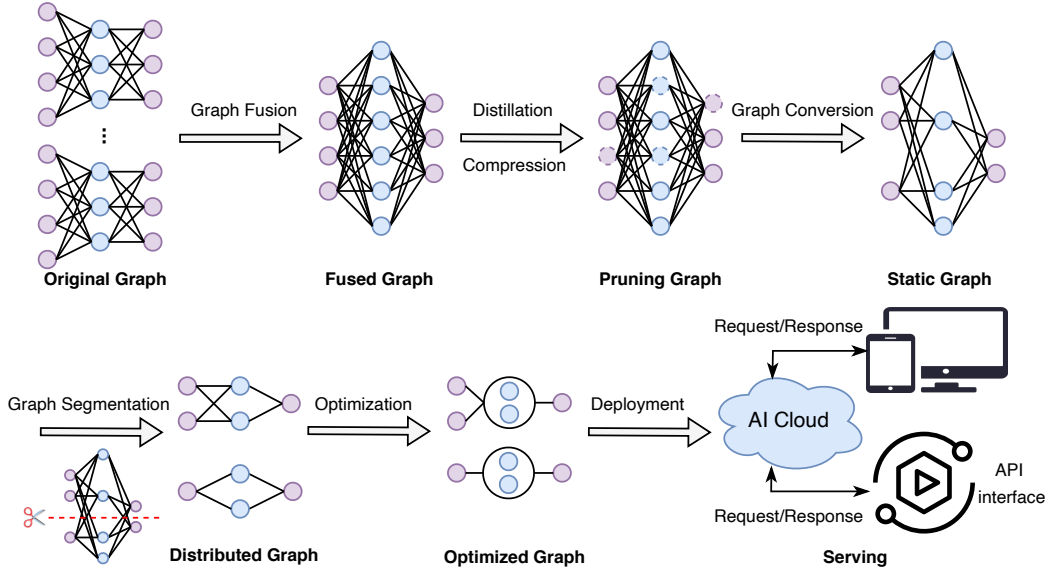


Figure 3: MoE Inference

It is worth mentioning that SE-MoE conjoins highly optimized transformers as well as MoE related kernels. We use the optimized methods that have been used in NVIDIA’s BERT implementation in MLPerf 1.1 [33] such as Fused Multi-head Attention, which is effective to reduce kernel launch time. For the MoE model, the unique kernels are made to improve H2D/D2H time by using CUDA Pinned Memory and customizing AlltoAll communication to minimize the number of layer transitions as much as possible. Specific inference performance experiment is shown in Section 5.2.

3.2 Ring Memory Offloading

To enable inference of a large-scale MoE model with limited resources, it is necessary to adopt the offloading strategy to solve the storage problem. Nevertheless, the speed of data movement inevitably becomes the bottleneck of inference performance. Therefore, many methods try to cover the data movement behind the inference calculation as much as possible, so that the calculation waiting time can be reduced. We design a dynamic scheduling strategy in offloading sparse parameters like expert parameters in the MoE model, trying to preserve efficient performance by overlapping the parameter movement from CPU memory and the inference computation in GPU memory.

As shown in Figure 4, each layer is independent of each other from the perspective of parameters in the MoE model like switch transformer architecture [16], which can be used to stagger computation and offloading to achieve overlap. Assuming there are N decoder layers in the MoE inference model, we store N copies of the expert parameters of N layers in the CPU device and put other parameters such as embeddings on the dense buffer of the GPU device. At the same time, the GPU device also caches K copies of the expert parameters. As shown in Figure 5a, once all the computation related to the i -th layer is finished, the corresponding P_i parameter in GPU memory can be released and start loading the S_{K+i} expert parameter of the $(K+i)$ -th layer from CPU memory asynchronously to occupy the space

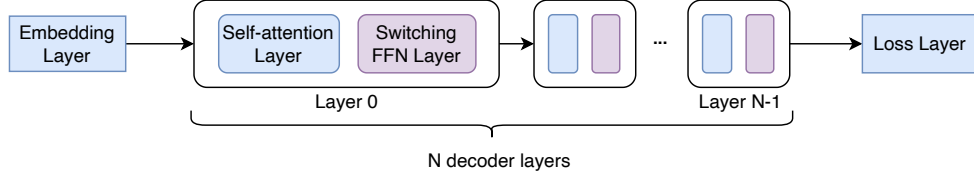


Figure 4: MoE Inference Model

of P_i . In this way, the fixed K copies of expert parameters on the GPU device are maintained by calculation-released-load, and they are stored in the ring memory to alleviate memory fragmentation. By using different CUDA streams, expert loading from CPU and computation can be partially overlapped, as illustrated in Figure 5b. And when the MoE inference model has more decoder layers and the ring memory size is sufficient, overlapping can be greatly maximized. Specific inference performance experiments using the ring memory are shown in Section 5.2.

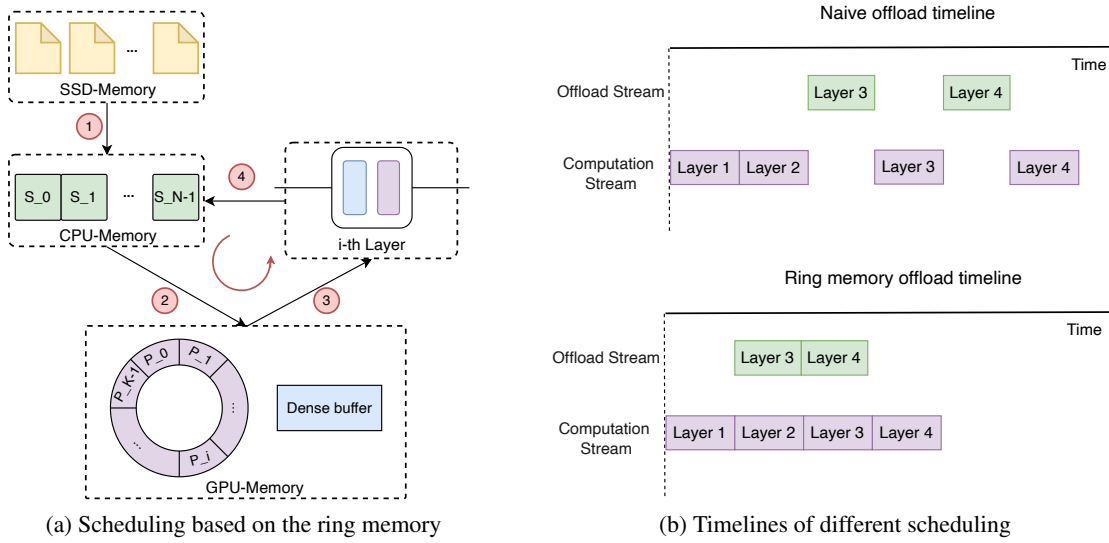


Figure 5: The scheduling and timeline of the ring memory offloading. The essential steps of scheduling: ① load N copies of parameters from files in SSD memory, ② load K copies of parameters from CPU memory, ③ execute the i -th layer computation, ④ release the i -th parameter and trigger asynchronous copy to replace P_i with S_{K+i} .

4 Efficient methods on MoE model

The unique architecture of the MoE model introduces new intrinsic problems in training and inference. The Elastic MoE Training has been designed to address the challenge of load imbalance due to uneven input data. Moreover, considering that MoE involves quite a bit of cross-machine communication, we explore Resource-aware Communication to speed up across different clusters. Finally, to overcome the limitation of storage because of the usage of oversized vocabulary in most tasks, we design and implement a novel embedding partition method in data parallelism, different from this in tensor-slicing parallelism.

4.1 Elastic MoE Training

The load imbalance largely affects the overall training performance, especially for multi-task training based on MoE architecture. For example, in the UFO task, due to the different amounts of input data on each task, the computing time is not uniform, causing serious load imbalance. On the one hand, the unbalanced load leads to the excess of the memory limit because the single task node processes a larger batch size due to the data collection from another node. On the other hand, synchronous communication has to wait for the slowest node which is known as the "Cask Effect" and results in a decline in computing utilization.

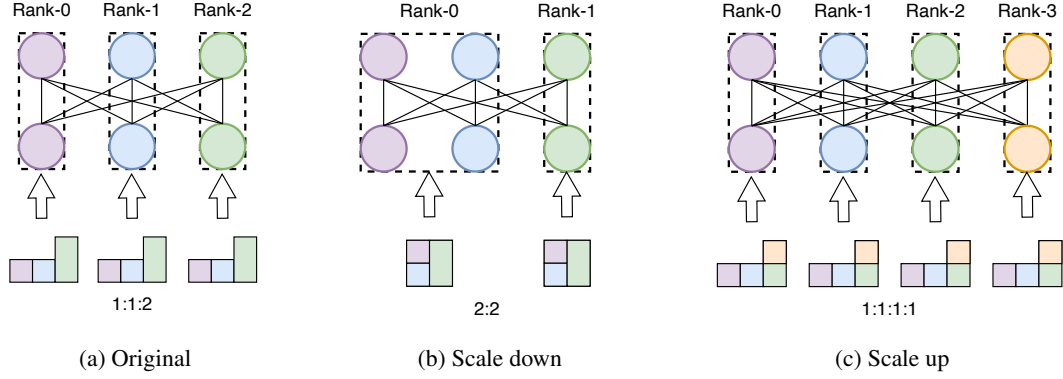


Figure 6: Different methods supported by elastic MoE training: (a) the original training with load imbalance, in which the ratio of each node data quantity is 1:1:2; (b) combining multiple nodes with light-duty tasks, in which the ratio of each node data quantity is 2:2; (c) adding extra nodes to handle heavy-duty tasks, in which the ratio of each node data quantity is 1:1:1:1.

According to the workload of the task that is statistically estimated in advance, the elastic MoE training method is taken to flexibly adjust the number of training nodes and ensure the load balance of each node. In general, combining multiple nodes with light-duty tasks can better utilize resources on the premise that storage is not the bottleneck as shown in Figure 6b. On the contrary, adding extra nodes to handle heavy-duty tasks reduces the workload as the same task is processed by more computing resources. At the same time, the input data of the heavy-duty task are divided to balance the input and the data parallelism is employed to ensure parameter synchronization as shown in Figure 6c. The above two methods of elastic training can effectively alleviate the performance degradation caused by unbalanced load and the specific performance comparison is shown in Section 5.3.

4.2 Resource-Aware Communication

During training and inference of the MoE model, a large amount of AlltoAll communication is required between devices in expert parallelism. It's possible to be a performance bottleneck and multiple processes of AlltoAll communication will compete for limited network resources at the same time. And after analyzing the network topology applied in our clusters, data interaction across clusters is much slower than devices within one cluster because of the larger message path and traffic cost.

Through NVLink, intra-node communication spends a small quantity of time and resources without crossing any Tor bridge or switch. However, when communication happens between different nodes in one cluster or across clusters, a larger message path crossing Tor bridges and switches is required and costs more time in traffic scheduling. Supposing that there are m clusters in the network and p nodes sharing the same series of Tor bridges in one cluster. All leaf switches (LE) and spin switches (SP) are divided into n and m groups respectively. As shown in Figure 7, leaf switches of the i -th group are connected directly to all Tor bridges only with rank i from different clusters. And the spin switches are used for interaction across leaf switches. Since the bandwidth of the spin switch is less than that of the leaf switch, data exchange should utilize leaf switch as much as possible for better performance. For example, supposing that all GPU0s are connected to $ToR1$ and all GPU7s are connected to $ToRn$, we see that data movement between GPU0 of Node1 from Cluster A and GPU7 of Node2 from Cluster B traverse through the switch routing path $[LE1, SPq, LE1]$ as marked by the red lines, which causes the larger cost of communication and the potential possibility of resource competition against other interactions. It's a better way to implement the above-mentioned communication by a two-step process with data movement from GPU0 to GPU7 in Node1 through NVLink, followed by cross-cluster communication between the pair of corresponding Tor bridges with rank 7 without crossing any switch except $LE1$, as marked by the blue lines. This enables full utilization of NVSwitch bandwidth and optimized network traffic.

Therefore, the data exchange speed of the same rank in node outperforms that of different rank in node. Based on the properties of the network topology, we suggest an optimized Hierarchical AlltoAll communication with resource awareness in training and inference. As shown in Figure 8, to avoid cross-node communication with different rank, we first implement intra-node AlltoAll through NVSwitch connection to gather the data. Then we categorize GPUs with the same rank into a group for inter-node AlltoAll and communicate across machines without unnecessary cost caused

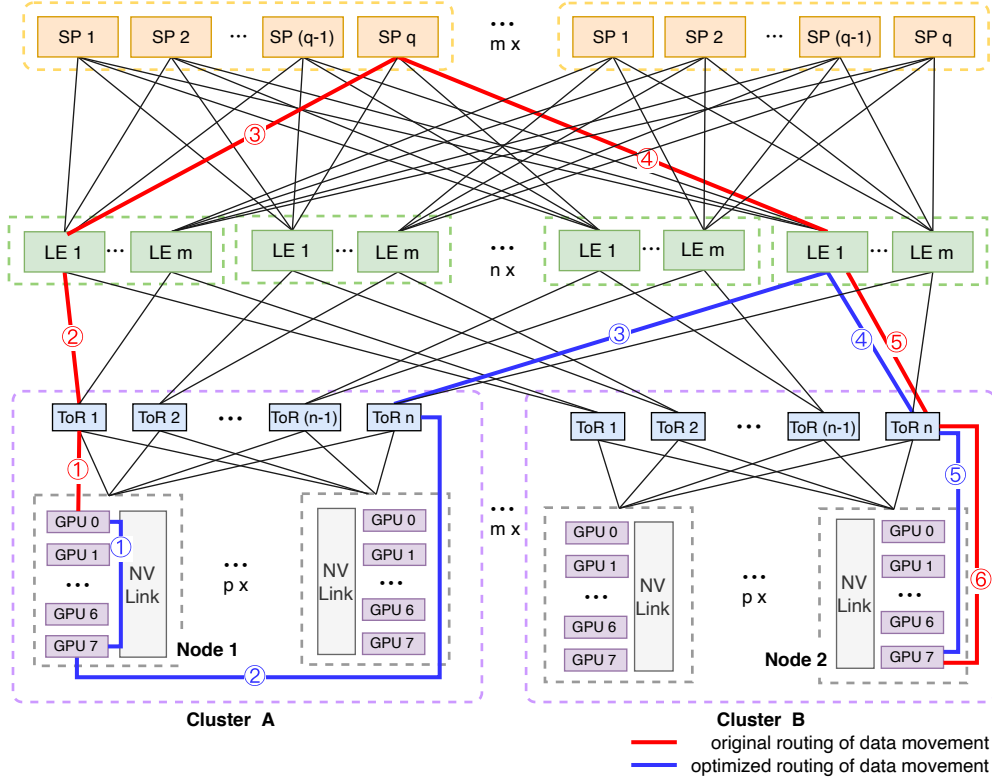


Figure 7: Network topology and message path of data movement

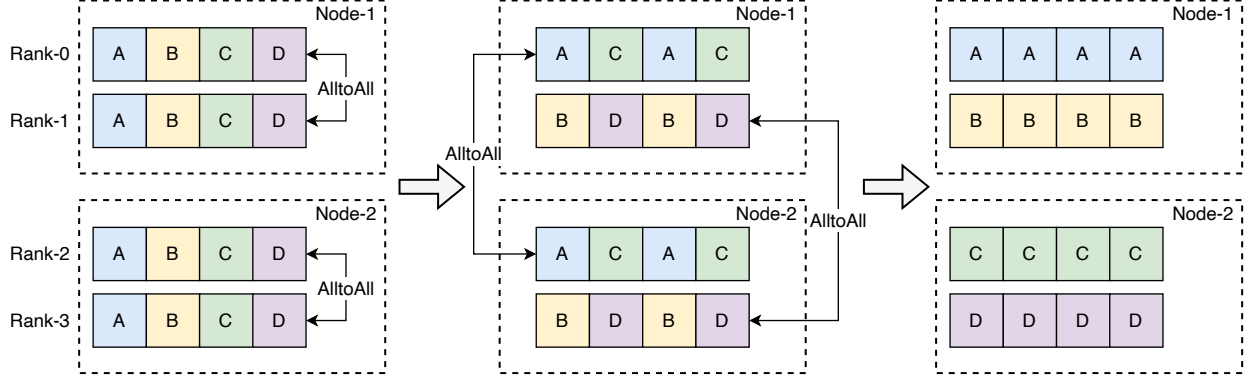


Figure 8: Hierarchical AlltoAll

by crossing rails. Besides, in this way, the peer-to-peer communication across nodes increased by a factor of p , where p is the number of GPUs in one node, which is capable of fully utilizing the inter-node bandwidth.

4.3 Embedding Partition in Data Parallelism

In the implementation of ultra-large-scale model training, the embedding table is often the largest parameter in the whole model parameters, so the storage of the embedding table is restricted to the model scale. There have been many works researching on the embedding partition. Megatron [34] has long applied the row-wise partitioned embedding table to tensor-slicing parallelism to reduce training memory, and EmbedRace [35] has proposed the column-wise partitioned method in the embedding table to achieve more balanced communication. However, there is no efficient processing way to deal with embedding partition when the input data of each process is inconsistent.

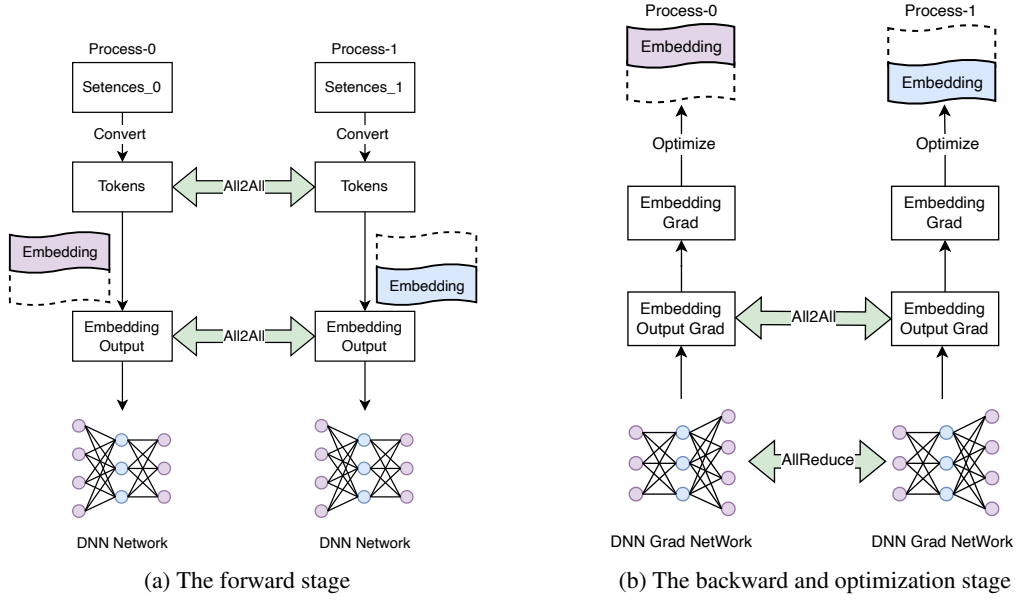


Figure 9: Example data flow of Embedding Partition in data parallelism. The embedding table is row-wise partitioned among processes. In the forward stage, AlltoAll communication is called twice: one is for exchanging input data and another is for exchanging embedding lookup results. In the backward stage, AlltoAll is called once to swap the gradient of the embedding table and using the gradients updates the embedding table.

As shown in Figure 9, in this work, we focus on embedding partition in data parallelism. Suppose we partition an embedding table with dimension $[V, H]$ among N training processes, the row-wise method distributed a $[\frac{V}{N}, H]$ shard to each worker, which means that every process only has an embedding representation of partial vocabulary. Therefore, before querying the embedding table, the input data of each process has to be exchanged with each other by AlltoAll communication to obtain the embedding results in the local partial vocabulary. Afterward, to obtain the correct results of the input data of the worker, the embedding results are exchanged again by AlltoAll communication which can be regarded as the inverse procedure of previous communication. Obviously, for the backward stage, the gradient is needed to exchange to recovery embedding table gradient. And unsurprisingly, it is an effective approach to reduce embedded table storage based on data parallelism, which introduces only three AlltoAll communications and remove AllReduce synchronization for embedding table gradients in data parallelism.

5 Experiment

In this section, we give a comprehensive evaluation of SE-MoE system using experiments about MoE models from the perspective of training and inference. First, the training efficiency is tested on GPT based on MoE architecture with different configurations. Next, the inference performance is measured and the offloading strategy based on ring memory is evaluated on the different model sizes. Lastly, taking the UFO model as an example, various efficient methods of SE-MoE are tested.

5.1 Large-Scale MoE Training

We train GPT models [2, 5] based on the MoE architecture on A100 GPUs(80 GB) by combining data parallelism and expert parallelism. Besides, we adopt Gshard [36] and top1-gating for evaluation. Simultaneously, we choose pure fp16 precision and the AdamW [37] optimizer for training. The results of throughput with different configurations are demonstrated in Table 1. From the table, compared with the state-of-the-art MoE system, DeepSpeed¹, SE-MoE obtains almost 28% speedup in single-node training and at least 33% speedup in multiple-node training for the MoE models with over-100-billions parameters. Meanwhile, SE-MoE decreases the employed GPU memory of each rank by nearly 12 GB.

¹<https://github.com/microsoft/Megatron-DeepSpeed>

Table 1: Results for MoE models on A100 GPUs in the different configurations

Parameters(B)	Attention heads	Hidden size	Vocab size	Layers	Experts	GPUs	Batch size	Speed(tokens/s)		Memory(GB)	
								DeepSpeed	SE-MoE	DeepSpeed	SE-MoE
13.9	64	4096	50304	12	8	8	8	24165	31085	68.9	56.8
26.8					16	16	16	43691	59136	66.2	53.9
52.6					32	32	32	82957	113456	66.8	54.5
104.1					64	64	64	157728	209970	66.3	54.4
207.2					128	128	128	283706	376968	66.4	54.3

5.2 MoE Inference

The experiments about inference include two parts: one shows the performance of the MoE inference system on the different models with billions of parameters, and the other one shows the effectiveness of the offloading strategy we propose in Section 3.2.

Effective Inference on MoE Substantially, inference requires less memory than training. So it’s easy to process downstream tasks with a 10-billion-parameter MoE model on a single GPU. We measure the inference performance of large-scale MoE models on the text generation task. As shown in Table 2, compared with DeepSpeed, SE-MoE obtains almost 13% speedup on MoE models with over 200 billion parameters.

Table 2: Results for performance of MoE inference on A100 GPUs

Parameters(B)	GPUs	Batch size	Speed(tokens/s)	
			DeepSpeed	SE-MoE
10.0	1	1	4303	4551
106.5	8	8	27215	29681
209.6	16	16	35310	40059

Ring Memory Offloading Using 16 A100(40G) GPUs in the experiment, we measure the inference performance of expert offloading strategy based on ring memory for the MoE model with 32 experts and 58.2B parameters. We also give the time of computation in GPU memory and expert movement from CPU memory. As shown in Figure 10, the performance of overlapped MoE inference system is almost unaffected by CPU offloading. According to the results, we see that this strategy can keep a relatively good balance between computation and data movement, and makes the MoE inference systems hold decreased GPU memory by at least 30% than inference without ring memory offloading.

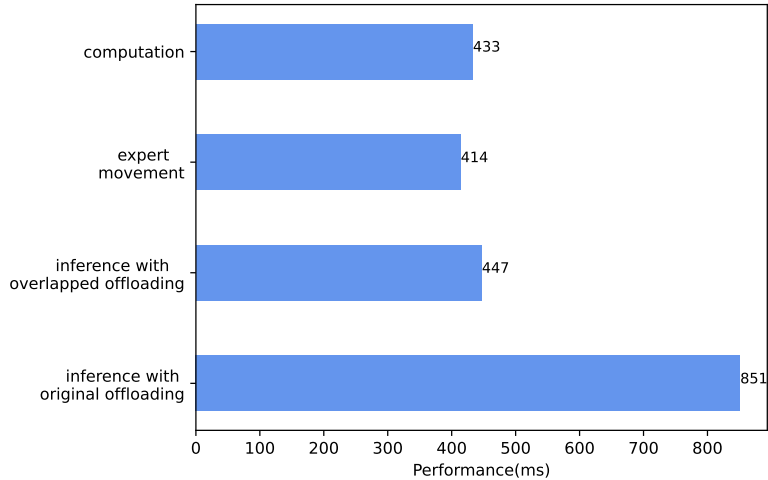


Figure 10: Performance of MoE inference w/ and w/o overlapped offloading

5.3 Multi-Task Training with MoE

The experiments below show the advantages of efficient methods on an actual large model, which are illustrated in Section 4.

Elastic MoE Training We train the UFO model on A100(80G) GPUs based on the MoE architecture to evaluate the efficiency of elastic MoE training. There are totally 4 tasks, and the batch size of each task is 512, 256, 128, and 128 respectively, which is imbalanced for training. By following the elastic sparse training described in Section 4.1, we adjust the entire training load by adding extra computing nodes, so that we choose 4 GPUs for Task-1 and 2 GPUs for Task-2. For the sake of fairness, we calculate the average speed of each GPU card for eliminating the impact caused by the increasing of nodes. As shown in Table 3, compared with load imbalance, the throughput of each card obtains 18.2% speedup.

Table 3: Results for elastic MoE training on A100 GPUs(80G)

	Task number	Parameters(M)	Total batch size	Batch size per task	GPUs	GPUs per task	Total Speed (samples/s)	Speed per card (samples/s)
Load imbalance	4	83	1024	512/256/128/128	4	1/1/1/1	250.4	62.6
Load balance					8	4/2/1/1	591.9	74.0

Resource-Aware Communication In this experiment, we train the MoE models on the different number of nodes and model sizes. From Figure 11, we see that after the Hierarchical AlltoAll training is adopted, the computation time does not increase significantly, but the communication time decreases dramatically. On the MoE model with 80.7B parameters in four nodes with 32 GPUs, the overall end-to-end training performance is improved by 10.3%, while the communication obtains speedup by 15.5% using Hierarchical AlltoAll.

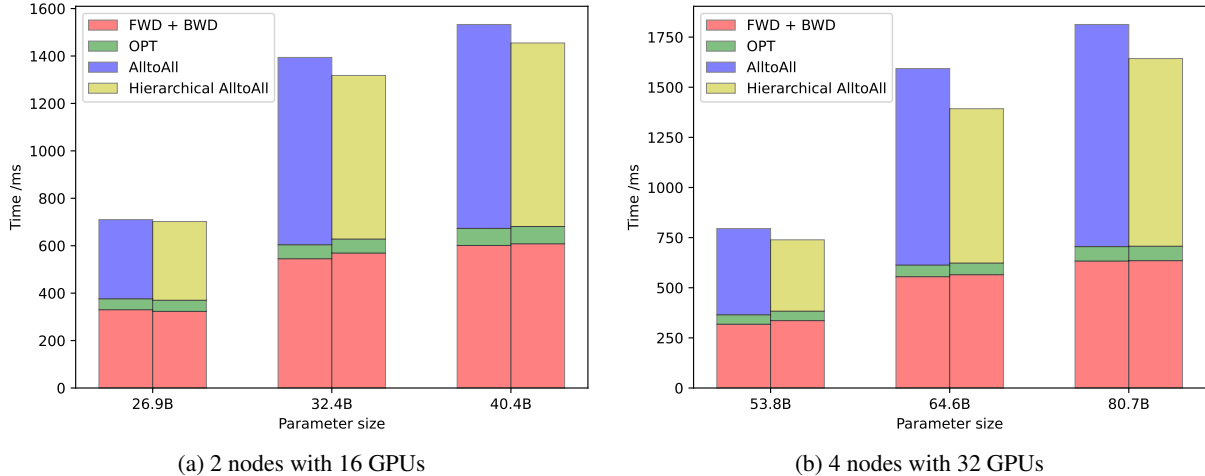


Figure 11: MoE Training Time Breakdown

Embedding Partition in Data Parallelism For the scene with a large vocabulary size, we train the MoE model with embedding partition in data parallelism. It can be seen from the experimental results that adopting embedding partition strategy in a single machine can effectively reduce the GPU memory consumption of large vocabulary size. Since each rank updates the partial vocabulary in parallel, the training performance will also be improved. As shown in Table 4, We take the non-segmented embedding under data parallelism as the baseline. With the increase of the hidden size, our method reduces GPU memory by 22.4%, 24.2% and 26.3%, while increasing the throughput by 4.2%, 11.2%, and 15.6% respectively.

Table 4: Embedding Partition in Data Parallelism on V100 GPUs

Batch size	GPUs	Experts	Vocab size	Hidden size	Parameter(M)	Memory (GB)		Speed (tokens/s)	
						Baseline	Embedding Partition	Baseline	Embedding Partition
8	8	8	50304	2048	100	7.46	5.78	144159	150161
				4096	300	12.80	9.70	86237	95890
				8192	700	27.80	20.49	40605	46938

6 Related Work

Sparsely Activated Models: Large-scale models based on Mixture-of-Experts have shown prominent advantages on natural language processing. Many papers [18, 36, 38] have focused on adapting the routing strategy to improve the model quality and performance. For low carbon and energy-saving, GLaM [17] has proved that the largest model with 1.2T parameters only consumes 1/3 of the energy used to train GPT-3.

Large-Scale Models with MoE There has been much research working on the increase of the model size for the last few years because of the scaling law [1]. Based on MoE architecture, billions and even trillions of models, like CPM-2 [39], M6-T [20], M6-10T [40], GLaM [17], are proved to have better generalization ability on natural language processing and multi-modal tasks. Besides, Baidu has proposed a unique UFO [41] based on MoE, which takes into account the deployment efficiency of large models and makes full use of big data and large models. With the introduction of the super network, the UFO model is composed of many subtasks, each of which is a path in the super network. One subtask is selected for training through the routing strategy.

MoE Training and Inference Systems: As the MoE training paradigm becomes popular, many scientific research institutions and enterprises have open-sourced MoE training frameworks and systems.

DeepSpeed-MoE [42, 32] utilizes a variety of distributed parallel methods to combine MoE parallelism, including data parallelism, tensor-slicing [34], ZeRO data parallelism [23] to train larger models. As for the inference of MoE, DeepSpeed designs a novel sparsely activated model named PR-MoE and model compression techniques to reduce MoE model size, and an efficient communication method to optimize latency [32].

FastMoE [19] is a distributed MoE training system to provide a hierarchical interface and simple institutions on how to use Megatron-LM [34] and Transformer-XL [43] based on data parallelism and tensor slicing parallelism. Different from the implementation of DeepSpeed, FastMoE utilizes a sophisticated optimized method to reduce network traffic. In addition, the inference system INFMoE [39] proposes the optimal order of computation and parameter offloading based on the greedy algorithm to address workload imbalance, aiming to fully conceal the cost of data movement caused by CPU-offloading and guarantee the efficiency of computation efficiency.

Fairseq-MoE [44, 28] is a sequence modeling framework to train the custom model for summarization, translation and language modeling. And Tutel [45] has further optimized the Fairseq system in communication and computing, whose performance has improved by about 40 percent. Moreover, the optimizations in Tutel have been integrated into DeepSpeed to facilitate MoE model training.

7 Conclusion and Future Work

This study demonstrates that SE-MoE, MoE training and inference system, can satisfy requirements well from NLP and CV tasks. It not only addresses the issue of large model about training and inference, but also achieves competitive performance. In the future, we will explore a unified sparse training and inference system that takes parameter-sever into account and scheduling in multiple dimensions. The unified system will be effective to improve sparse training to overcome communication, computing and storage bottlenecks. Besides, how to utilize sparse training for large scale models to obtain better convergence in various tasks is still a seductive topic. We will further research efficient methods for sparse training of SE-MoE. At last, we will enhance our unified system by collaborating with the resource platform to perform lower carbon and more environmentally friendly research.

References

- [1] Jared Kaplan, Sam McCandlish, Tom Henighan, Tom B Brown, Benjamin Chess, Rewon Child, Scott Gray, Alec Radford, Jeffrey Wu, and Dario Amodei. Scaling laws for neural language models. *arXiv preprint arXiv:2001.08361*, 2020.

- [2] Tom Brown, Benjamin Mann, Nick Ryder, Melanie Subbiah, Jared D Kaplan, Prafulla Dhariwal, Arvind Neelakantan, Pranav Shyam, Girish Sastry, Amanda Askell, et al. Language models are few-shot learners. *Advances in neural information processing systems*, 33:1877–1901, 2020.
- [3] Jacob Devlin, Ming-Wei Chang, Kenton Lee, and Kristina Toutanova. Bert: Pre-training of deep bidirectional transformers for language understanding. *arXiv preprint arXiv:1810.04805*, 2018.
- [4] Alexey Dosovitskiy, Lucas Beyer, Alexander Kolesnikov, Dirk Weissenborn, Xiaohua Zhai, Thomas Unterthiner, Mostafa Dehghani, Matthias Minderer, Georg Heigold, Sylvain Gelly, et al. An image is worth 16x16 words: Transformers for image recognition at scale. *arXiv preprint arXiv:2010.11929*, 2020.
- [5] Deepak Narayanan, Mohammad Shoeybi, Jared Casper, Patrick LeGresley, Mostofa Patwary, Vijay Korthikanti, Dmitri Vainbrand, Prethvi Kashinkunti, Julie Bernauer, Bryan Catanzaro, et al. Efficient large-scale language model training on gpu clusters using megatron-lm. In *Proceedings of the International Conference for High Performance Computing, Networking, Storage and Analysis*, pages 1–15, 2021.
- [6] Shuohuan Wang, Yu Sun, Yang Xiang, Zhihua Wu, Siyu Ding, Weibao Gong, Shikun Feng, Junyuan Shang, Yanbin Zhao, Chao Pang, et al. Ernie 3.0 titan: Exploring larger-scale knowledge enhanced pre-training for language understanding and generation. *arXiv preprint arXiv:2112.12731*, 2021.
- [7] Shaden Smith, Mostofa Patwary, Brandon Norick, Patrick LeGresley, Samyam Rajbhandari, Jared Casper, Zhun Liu, Shrimai Prabhumoye, George Zerveas, Vijay Korthikanti, et al. Using deepspeed and megatron to train megatron-turing nlg 530b, a large-scale generative language model. *arXiv preprint arXiv:2201.11990*, 2022.
- [8] Weijie Zhao, Jingyuan Zhang, Deping Xie, Yulei Qian, Ronglai Jia, and Ping Li. Aibox: Ctr prediction model training on a single node. In *Proceedings of the 28th ACM International Conference on Information and Knowledge Management*, pages 319–328, 2019.
- [9] Weijie Zhao, Deping Xie, Ronglai Jia, Yulei Qian, Ruiquan Ding, Mingming Sun, and Ping Li. Distributed hierarchical gpu parameter server for massive scale deep learning ads systems. *Proceedings of Machine Learning and Systems*, 2:412–428, 2020.
- [10] Rich Caruana. Multitask learning. *Machine learning*, 28(1):41–75, 1997.
- [11] Linting Xue, Noah Constant, Adam Roberts, Mihir Kale, Rami Al-Rfou, Aditya Siddhant, Aditya Barua, and Colin Raffel. mT5: A massively multilingual pre-trained text-to-text transformer. In *Proceedings of the 2021 Conference of the North American Chapter of the Association for Computational Linguistics: Human Language Technologies*, pages 483–498, Online, June 2021. Association for Computational Linguistics. doi: 10.18653/v1/2021.naacl-main.41. URL <https://aclanthology.org/2021.naacl-main.41>.
- [12] Roei Aharoni, Melvin Johnson, and Orhan Firat. Massively multilingual neural machine translation. In *Proceedings of the 2019 Conference of the North American Chapter of the Association for Computational Linguistics: Human Language Technologies, Volume 1 (Long and Short Papers)*, pages 3874–3884, Minneapolis, Minnesota, June 2019. Association for Computational Linguistics. doi: 10.18653/v1/N19-1388. URL <https://aclanthology.org/N19-1388>.
- [13] Yiren Wang, ChengXiang Zhai, and Hany Hassan. Multi-task learning for multilingual neural machine translation. In *Proceedings of the 2020 Conference on Empirical Methods in Natural Language Processing (EMNLP)*, pages 1022–1034, Online, November 2020. Association for Computational Linguistics. doi: 10.18653/v1/2020.emnlp-main.75. URL <https://aclanthology.org/2020.emnlp-main.75>.
- [14] Noam Shazeer, Azalia Mirhoseini, Krzysztof Maziarz, Andy Davis, Quoc Le, Geoffrey Hinton, and Jeff Dean. Outrageously large neural networks: The sparsely-gated mixture-of-experts layer. *arXiv preprint arXiv:1701.06538*, 2017.
- [15] Dmitry Lepikhin, Hyoungho Lee, Yuanzhong Xu, Dehao Chen, Orhan Firat, Yanping Huang, Maxim Krikun, Noam Shazeer, and Zhifeng Chen. Gshard: Scaling giant models with conditional computation and automatic sharding. *arXiv preprint arXiv:2006.16668*, 2020.
- [16] William Fedus, Barret Zoph, and Noam Shazeer. Switch transformers: Scaling to trillion parameter models with simple and efficient sparsity. *arXiv preprint arXiv:2101.03961*, 2021.
- [17] Nan Du, Yanping Huang, Andrew M Dai, Simon Tong, Dmitry Lepikhin, Yuanzhong Xu, Maxim Krikun, Yanqi Zhou, Adams Wei Yu, Orhan Firat, et al. Glam: Efficient scaling of language models with mixture-of-experts. *arXiv preprint arXiv:2112.06905*, 2021.
- [18] Simiao Zuo, Xiaodong Liu, Jian Jiao, Young Jin Kim, Hany Hassan, Ruofei Zhang, Tuo Zhao, and Jianfeng Gao. Taming sparsely activated transformer with stochastic experts. *arXiv preprint arXiv:2110.04260*, 2021.
- [19] Jiaao He, Jiezhong Qiu, Aohan Zeng, Zhilin Yang, Jidong Zhai, and Jie Tang. Fastmoe: A fast mixture-of-expert training system. *arXiv preprint arXiv:2103.13262*, 2021.
- [20] An Yang, Junyang Lin, Rui Men, Chang Zhou, Le Jiang, Xianyan Jia, Ang Wang, Jie Zhang, Jiamang Wang, Yong Li, et al. M6-t: Exploring sparse expert models and beyond. *arXiv preprint arXiv:2105.15082*, 2021.
- [21] Stephen W Keckler, William J Dally, Bruce Khailany, Michael Garland, and David Glasco. Gpus and the future of parallel computing. *IEEE micro*, 31(5):7–17, 2011.

- [22] Samyam Rajbhandari, Olatunji Ruwase, Jeff Rasley, Shaden Smith, and Yuxiong He. Zero-infinity: Breaking the gpu memory wall for extreme scale deep learning. In *Proceedings of the International Conference for High Performance Computing, Networking, Storage and Analysis*, pages 1–14, 2021.
- [23] Samyam Rajbhandari, Jeff Rasley, Olatunji Ruwase, and Yuxiong He. Zero: Memory optimizations toward training trillion parameter models. In *SC20: International Conference for High Performance Computing, Networking, Storage and Analysis*, pages 1–16. IEEE, 2020.
- [24] wikipedia. Solid-state drive. https://en.wikipedia.org/wiki/Solid-state_drive, 2022.
- [25] Diederik P Kingma and Jimmy Ba. Adam: A method for stochastic optimization. *arXiv preprint arXiv:1412.6980*, 2014.
- [26] Intel. Memory optimized for data-centric workloads. <https://www.intel.cn/content/www/cn/zh/architecture-and-technology/optane-dc-persistent-memory.html>, 2018.
- [27] Leonid B Sokolinsky. Lfu-k: An effective buffer management replacement algorithm. In *International Conference on Database Systems for Advanced Applications*, pages 670–681. Springer, 2004.
- [28] Mikel Artetxe, Shruti Bhosale, Naman Goyal, Todor Mihaylov, Myle Ott, Sam Shleifer, Xi Victoria Lin, Jingfei Du, Srinivasan Iyer, Ramakanth Pasunuru, et al. Efficient large scale language modeling with mixtures of experts. *arXiv preprint arXiv:2112.10684*, 2021.
- [29] Geoffrey Hinton, Oriol Vinyals, Jeff Dean, et al. Distilling the knowledge in a neural network. *arXiv preprint arXiv:1503.02531*, 2(7), 2015.
- [30] Sam Shleifer and Alexander M Rush. Pre-trained summarization distillation. *arXiv preprint arXiv:2010.13002*, 2020.
- [31] Victor Sanh, Lysandre Debut, Julien Chaumond, and Thomas Wolf. Distilbert, a distilled version of bert: smaller, faster, cheaper and lighter. *arXiv preprint arXiv:1910.01108*, 2019.
- [32] Samyam Rajbhandari, Conglong Li, Zhewei Yao, Minjia Zhang, Reza Yazdani Aminabadi, Ammar Ahmad Awan, Jeff Rasley, and Yuxiong He. Deepspeed-moe: Advancing mixture-of-experts inference and training to power next-generation ai scale. *arXiv preprint arXiv:2201.05596*, 2022.
- [33] Peter Mattson, Christine Cheng, Gregory Diamos, Cody Coleman, Paulius Micikevicius, David Patterson, Hanlin Tang, Gu-Yeon Wei, Peter Bailis, Victor Bittorf, et al. Mlperf training benchmark. *Proceedings of Machine Learning and Systems*, 2: 336–349, 2020.
- [34] Mohammad Shoeybi, Mostofa Patwary, Raul Puri, Patrick LeGresley, Jared Casper, and Bryan Catanzaro. Megatron-lm: Training multi-billion parameter language models using model parallelism. *arXiv preprint arXiv:1909.08053*, 2019.
- [35] Shengwei Li, Zhiquan Lai, Dongsheng Li, Xiangyu Ye, and Yabo Duan. Embrace: Accelerating sparse communication for distributed training of nlp neural networks. *arXiv preprint arXiv:2110.09132*, 2021.
- [36] Sam Gross, Marc’Aurelio Ranzato, and Arthur Szlam. Hard mixtures of experts for large scale weakly supervised vision. In *Proceedings of the IEEE Conference on Computer Vision and Pattern Recognition*, pages 6865–6873, 2017.
- [37] Ilya Loshchilov and Frank Hutter. Decoupled weight decay regularization. In *International Conference on Learning Representations*, 2018.
- [38] Mike Lewis, Shruti Bhosale, Tim Dettmers, Naman Goyal, and Luke Zettlemoyer. Base layers: Simplifying training of large, sparse models. In *International Conference on Machine Learning*, pages 6265–6274. PMLR, 2021.
- [39] Zhengyan Zhang, Yuxian Gu, Xu Han, Shengqi Chen, Chaojun Xiao, Zhenbo Sun, Yuan Yao, Fanchao Qi, Jian Guan, Pei Ke, et al. Cpm-2: Large-scale cost-effective pre-trained language models. *AI Open*, 2:216–224, 2021.
- [40] Junyang Lin, An Yang, Jinze Bai, Chang Zhou, Le Jiang, Xianyan Jia, Ang Wang, Jie Zhang, Yong Li, Wei Lin, et al. M6-10t: A sharing-delinking paradigm for efficient multi-trillion parameter pretraining. *arXiv preprint arXiv:2110.03888*, 2021.
- [41] Baidu. A new paradigm of large model application: unified feature representation optimization. <https://mp.weixin.qq.com/s/GgPrDJwYsvRSWQ0D3LgI3w>, 2022.
- [42] Young Jin Kim, Ammar Ahmad Awan, Alexandre Muzio, Andres Felipe Cruz Salinas, Liyang Lu, Amr Hendy, Samyam Rajbhandari, Yuxiong He, and Hany Hassan Awadalla. Scalable and efficient moe training for multitask multilingual models. *arXiv preprint arXiv:2109.10465*, 2021.
- [43] Zihang Dai, Zhilin Yang, Yiming Yang, Jaime Carbonell, Quoc V Le, and Ruslan Salakhutdinov. Transformer-xl: Attentive language models beyond a fixed-length context. *arXiv preprint arXiv:1901.02860*, 2019.
- [44] Myle Ott, Sergey Edunov, Alexei Baevski, Angela Fan, Sam Gross, Nathan Ng, David Grangier, and Michael Auli. fairseq: A fast, extensible toolkit for sequence modeling. In *Proceedings of NAACL-HLT 2019: Demonstrations*, 2019.
- [45] Microsoft. Tutel: An efficient mixture-of-experts implementation for large dnn model training. <https://www.microsoft.com/en-us/research/blog/tutel-an-efficient-mixture-of-experts-implementation-for-large-dnn-model-training/>, 2021.